

TSC Simulation of Transient CHI in New Electrode Configuration on QUEST^{*)}

Kengoh KURODA, Roger RAMAN¹⁾, Stephen C. JARDIN²⁾, Masayuki ONO²⁾ and Kazuaki HANADA

Kyushu University, Kasuga, Fukuoka 816-8580, Japan

¹⁾*University of Washington, Seattle, WA, 98195, USA*

²⁾*Princeton Plasma Physics Laboratory, Princeton, NJ, 08543, USA*

(Received 27 December 2017 / Accepted 15 April 2018)

In QUEST, *transient* Coaxial Helicity Injection (CHI) has now been implemented using a new electrode configuration in which the CHI insulator is not part of the vacuum boundary. In this paper, for the first time, suitable conditions for generation of the CHI-produced toroidal current in the QUEST vessel configuration were investigated using the Tokamak Simulation Code (TSC). The simulation results show that the configuration in which the biased electrode is located farther away from the injector flux coil requires higher currents in the injector coil to generate the required injector flux. Additionally, energizing a lower inboard poloidal field coil and possibly lowering the electrode plate closer to the injector flux coil may be necessary to improve injector flux shaping to permit a configuration that is more favorable for inducing flux closure.

© 2018 The Japan Society of Plasma Science and Nuclear Fusion Research

Keywords: CHI, TSC, non-inductive current drive, spherical tokamak, ECH

DOI: 10.1585/pfr.13.3402059

1. Introduction

Transient Coaxial Helicity Injection (CHI) is a useful method to generate plasma current without the use of a solenoid in a low aspect ratio spherical tokamak (ST) device as it has the advantages of low construction cost and high plasma beta which is desired in a future fusion reactor. On the HIT-II experiment at the University of Washington, the method referred to as *transient* CHI was developed, which generated toroidal plasma currents accompanied by the formation of closed-flux surfaces. These plasmas were subsequently ramped up to 290 kA using inductive drive that consumed less solenoid flux compared to discharges without CHI start-up [1]. The method was further developed on the NSTX device at the Princeton Plasma Physics Laboratory (PPPL) where a CHI produced plasma current of about 200 kA was ramped up to 1 MA by using only 65 % of the solenoid flux of a discharge with full inductive drive [2].

In the mid-size ST device, QUEST [3,4], we have now implemented *transient* CHI capability through a collaborative research with the University of Washington and PPPL [5]. The main objectives of this experiment are the demonstration of generating CHI plasma using a new, much more reactor-relevant, electrode configuration and the investigation of the efficiency of CHI coupling to electron cyclotron resonance heating (ECH). The new electrode configuration, shown in Fig. 1, is designed to facilitate easier im-

plementation of CHI in future fusion reactors [6]. In this configuration the insulator is sandwiched between the bias electrode plate and the lower divertor plate, and it is not part of the vessel vacuum boundary as in NSTX and HIT-II. In this configuration, it is easier to shield the insulator from neutrons in a burning plasma device. Additionally, transient CHI plasmas have low intrinsic electron temperature, and they must be heated to the 1 keV temperature range for coupling to other non-inductive current sustainment methods [7]. ECH is a very powerful tool for heating low-temperature plasmas. Demonstrating electron heating of a transient CHI target using the high power 28 GHz ECH system on QUEST is an important objective [8].

In experiments thus far, we have achieved reliable gas breakdown [5] and good CHI plasma evolution. Demonstration of the formation of closed-flux surfaces is the next important objective. In support of this objective, the Tokamak Simulation Code (TSC) [9, 10] was used to understand the required PF coil programming to achieve desirable toroidal current evolution into the QUEST vessel that is favorable for a formation of flux closure.

The TSC code was developed at PPPL [9, 10] for simulating inductive tokamak plasma discharges. It simulates axisymmetric and free-boundary tokamak plasmas. In the code, information related to vessel and poloidal field coil (PF) parameters need to be provided as input. The required information is the vessel and coil shape and size as well as the resistance of all conductors. For the PF coils, the number of turns in the coil also needs to be provided. In

author's e-mail: kuroda@triam.kyushu-u.ac.jp

^{*)} This article is based on the presentation at the 26th International Toki Conference (ITC26).

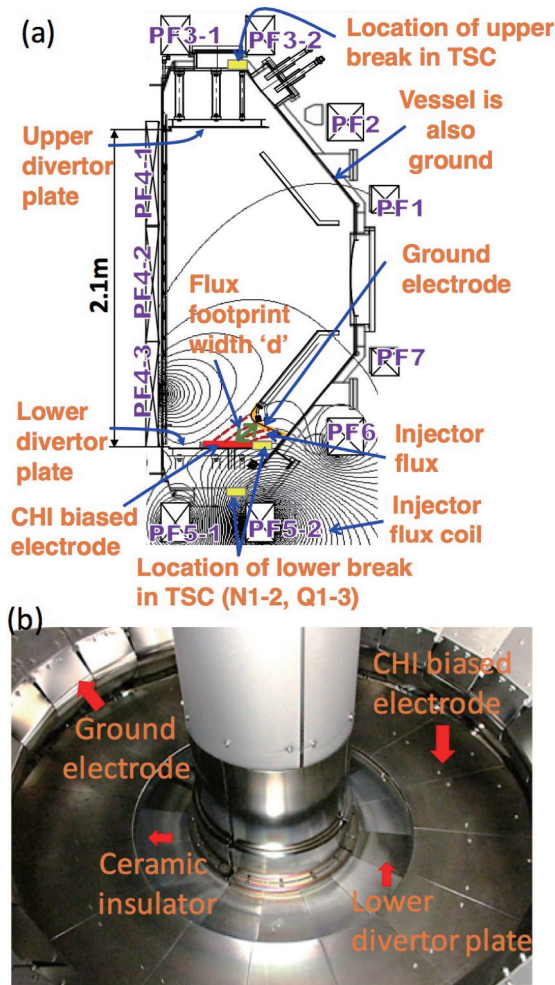


Fig. 1 CHI components on QUEST – the biased CHI electrode shown in red is positioned above the lower divertor plate. (b) Photo of CHI electrodes in QUEST. Reprinted with permission from [5].

addition, basic information about the plasma parameters are included. For simulating CHI discharges, the plasma electron temperature is used to calculate the Spitzer resistivity. The code then solves the MHD/Maxwell's equations and the circuit equations for the Poloidal Field coils. The region inside a rectangular computational grid is solved with finite difference equations, and a Green's function approach extends the solution to infinity.

2. TSC Simulations

In these first simulations of the QUEST CHI configuration, to touch base with previous such simulations for NSTX [11], we first studied the impact of moving the CHI electrodes farther away from the injector flux coil (as on QUEST), vs. closer positioning of the electrodes to the injector flux coil (as on NSTX). Five configurations were studied, as described in Table 1.

In Table 1, the 'N' electrode location refers to the electrode plates located closer to the injector flux coil, while the 'Q' configuration refers to the plates being lifted up

Table 1 Simulated discharge conditions.

	N1	N2	Q1	Q2	Q3
Electrode location	Low	Low	Lift up	Lift up	Lift up
Injector flux coil (PF5-2) current [kA]	0.4 →0.	0.4 →0.	3.0 →0.	3.0 →0.	3.0 →0.
Electron Temperature [eV]	200	200	200	100	50
Injector flux [mWb]	5	5	25	25	25
Injector voltage [V]	120 →0.	120 →0.	66 →0.	70 →0.	78 →0.

from the injector flux coil and located farther away from the coil, as on QUEST. A comparison of the lower vessel boundary on Figs. 2 and 3 shows the difference between the 'N' and 'Q' configurations. In Table 1, the terms 'Low' and 'Lift up' are used to identify these two configurations. The injector flux coil current is the current driven in the injector coil PF5-2 to generate the required injector flux. In configuration N1, starting from an initial value, the current in the injector coil is rapidly ramped down in time, while in configuration N2 the coil current is held constant in time. In the 'Q' configurations the electron temperature and the applied voltage are varied, as shown in Table 1. The injector flux is the magnitude of poloidal injector flux that connects the two electrodes, electron temperature is the temperature of the plasma used in the simulations, and the injector voltage is the voltage applied to the electrodes. In all cases, the toroidal coil current is 800 kA.

TSC was developed primarily for simulating axisymmetric inductive plasmas. While it has been used to support CHI experimental activities, it is not meant to exactly duplicate the experiment. Instead it is used as a guide for experiments to understand how the evolving CHI plasma can be controlled by appropriate choice of the poloidal field coil currents. Thus, TSC cannot be used to determine the exact value of closed flux current that can be generated in a given CHI configuration, but it can help one gain an understanding of configurations that can likely help optimize closed flux formation. The detailed aspects of closed flux current generation require a 3-d resistive MHD code such as NIMROD [12, 13]. Specifically, for QUEST, these initial TSC simulations have already helped us identify the need for energizing an additional PF coil to improve the CHI plasma evolution. In simulating QUEST CHI discharges, the vessel model is simplified to reproduce the most important parameters needed to model the poloidal flux evolution. These are the physical location of the CHI electrode area in relation to the PF coils, and the PF coil and vessel parameters. To have confidence that these simulations are meaningful, we also simulated a case in which the vessel configuration looks similar to the NSTX vessel configuration, and a configuration that has been previously studied using the TSC code [11]. In Table 1, these are

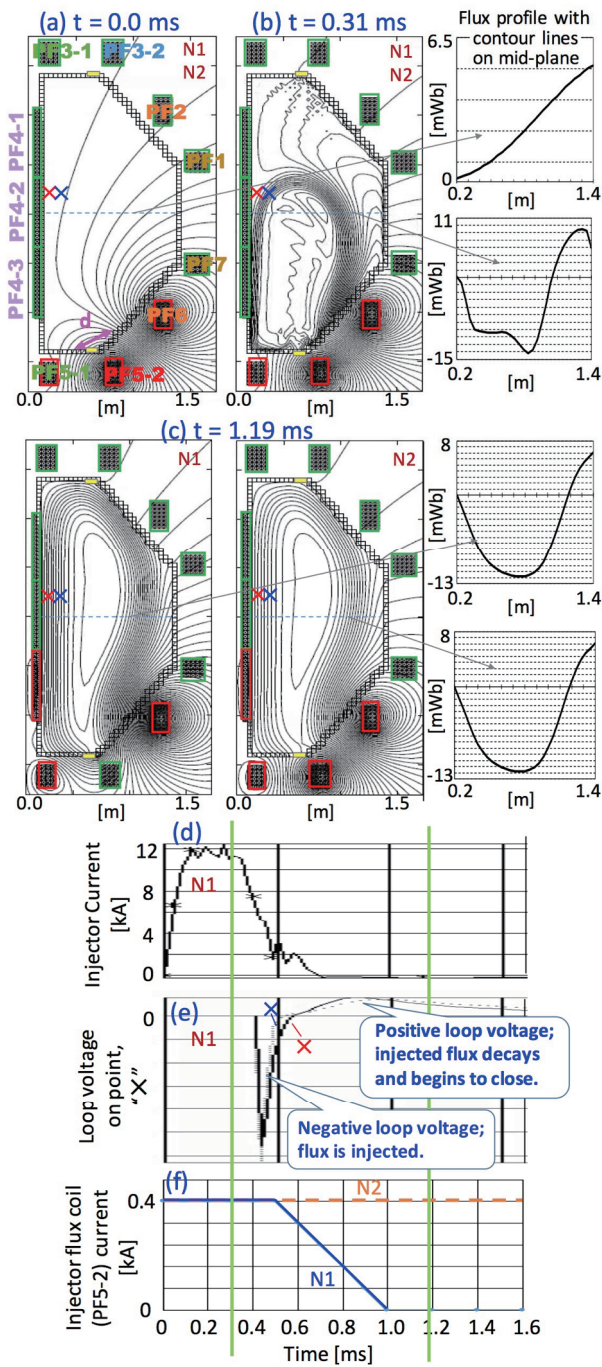


Fig. 2 Simulated results for cases N1 and N2, (a) - (c); flux evolution at three different times and the poloidal flux at $z = 0$. Current is driven in PF coils shown in red color. "d" is the flux footprint width. (d), (e); time plot of injector current and loop voltage at the two locations marked with an X in (a) - (c), (f); programed time plot of PF5-2 injector flux coil current.

identified with labels 'N' and 'Q' to represent the NSTX and QUEST-like configurations. The simulation area covers the region of the PF coils and the vacuum vessel. This entire area is modeled as small rectangular grids with a cross-section of $4\text{ cm} \times 4\text{ cm}$ each. At each of these grid locations the resistivity of the region is specified. To sim-

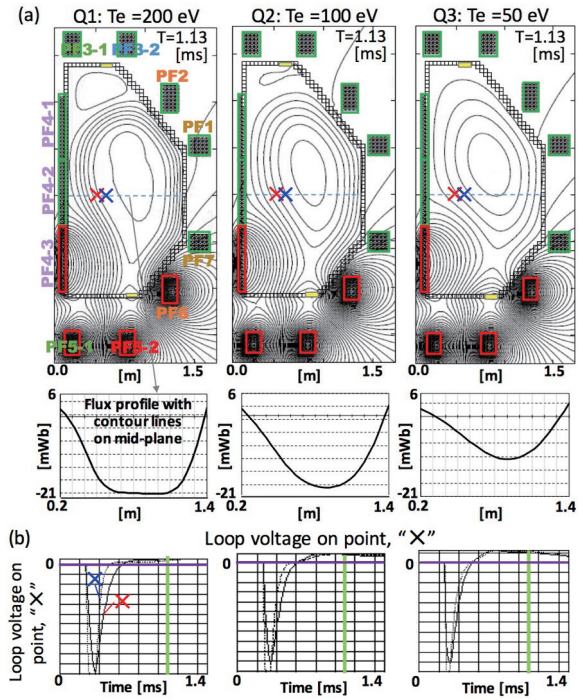


Fig. 3 Simulated results for configurations Q1-Q3 in which the electron temperature is changed, (a) flux evolution, (b) time plot of loop voltage at location X.

ulate CHI, in the lower part of the vessel a small region corresponding to the approximate location of the vacuum gap between the anode and cathode electrodes is specified to have very high resistance, like that of an insulator. A yellow rectangle on the lower part of the vessel in Fig. 1 (a) shows the insulator gap. The TSC model requires the need for a second insulator to avoid current from flowing along the QUEST vessel walls. In this model, this is located on the top of the vessel as shown by another yellow rectangle as in NSTX. The injector flux is located on either side of the high resistance gap on the lower part of the vessel, in which voltage is applied to either side of the gap. The applied voltage causes currents to flow along the initial vacuum flux that is present on either side of this gap, which adequately simulates the actual current flowing between the bias and ground electrodes. The electron temperature in Table 1 is used to prescribe a resistivity profile for the magnetic flux region. As currents flow along these field lines, a $\mathbf{J} \times \mathbf{B}$ force is generated that causes the poloidal flux to evolve into the vessel region. Currents driven in the PF coils then determine the shape of the evolving CHI plasma discharge, as shown in Figs. 2 and 3.

In CHI terminology, the average distance between the two injector flux footprints on the electrodes is the flux footprint width, 'd'. While the vacuum gap distance sets a lower value for the injector flux footprint width, the actual value for 'd' is determined by how much the injector flux footprint itself is spread out on the electrode surface, as shown in Fig. 2 (a). By increasing the current in the coils

adjacent to the main injector coil, the value of 'd' can be reduced and made narrower.

Figure 2 shows the simulated results for configuration N1. In this case, the CHI electrode is located closer to the injector flux coils. The initial PF configuration in (a), at $t = 0$ s, shows the shape of the vacuum injector flux. 5 mWb of injector flux forms the injector current path, and it is generated by using only 0.4 kA of current in the injector flux coil PF5-2. The Peak injector voltage is 120 V. The time-dependent voltage for all cases is applied in the same way. It increases from 0 V at $t = 0$ ms to a peak value at 0.2 ms. It is held at the peak value for 0.1 ms, then it is decreased back to 0 V at $t = 0.7$ ms. With the application of the voltage, the injector current flows along helical field lines formed by the combination of the injector flux and the toroidal field. With increasing injector current, as shown in (b), the injector flux expands into vessel when the interaction force between the injector current and toroidal field generated by the injector current exceeds the tension of the injector flux field lines [14]. After the injected flux fills the vessel, the time plot (d) shows that the injector current decreases rapidly because the injector voltage is reduced. This causes the injected flux to decay in time, inducing a positive loop voltage in the plasma region. The plot of the loop voltage (e) shows that it is negative as poloidal flux is injected into the vessel, but later in time becomes positive as the injected flux decays. Generation of closed flux in TSC simulations of CHI is due to this positive loop voltage generation by the decaying injected flux.

The conditions for case N2 are the same as the conditions in case N1 except that the current in the PF5-2 coil is kept constant in time, whereas for case N1 it is decreased to 0 Amp after the flux injection phase, as shown in Fig. 2 (f). However, the results for case N2 show similar flux evolution and closed flux formation as N1. This suggests that the rapidly reducing injector current is more important than the role of PF5-2 coil current ramp-down for inducing a positive loop voltage that is necessary in the TSC model for inducing the initial flux closure.

To clarify, in comparing cases N1 and N2, we note that there are two loop voltages. First is the loop voltage produced due to the changing current in the injector coil. In case N2, this is zero because the current in the injector coil PF5-2 is not changed in time. In case N1, it is positive because the current in this coil is decreasing in time. But this does not seem to result in significantly increased initial flux closure probably because the coil is far away from the central plasma region. Second is the loop voltage induced by the decaying open poloidal flux that has already been injected into the vessel during the CHI start-up process. For this flux, the action of driving open-field line current provides the $\mathbf{J} \times \mathbf{B}$ force necessary to keep it stretched inside the vessel. Once this open field line current drive has been removed (by rapidly reducing the injector voltage), then this injected flux can no longer remain in the vessel, and it will start to pull back into the injector. It is the decay

of this flux that generates the positive loop voltage needed for flux closure. If the injector flux footprint width is narrow, then that would make it much more difficult for the poloidal flux in the vessel to fully pull back into the injector region, and a greater amount of the injected open flux can close to form a closed flux configuration.

In cases Q1-3, the bias electrode is lifted up to the location corresponding to that on QUEST, as shown in Fig. 3. In this electrode configuration, the PF5-2 coil current is increased to 3.0 kA to produce 25 mWb of injector flux. Because the region of the high magnetic flux density is at larger major radius for this configuration, relatively high currents are also needed in the PF4-3 and PF5-1 coils as otherwise the injector flux is spread-out over a large electrode area making the injector flux footprint width large. Driving currents in these coils causes the injector flux to be more concentrated near the gap region that is above the PF5-2 coil. Under these conditions the injector flux is more concentrated near the electrode gap region, as for case N, and flux closure is also seen in this configuration, as shown in Fig. 3. These cases require less voltage because, in general, the injector flux can be thought of as shorting the electrodes. So with other factors remaining the same, a higher value of the injector flux requires less voltage to obtain a given value of injector current that is consistent with plasma growth that fills the vessel [11]. It is also useful to note that the magnitude of the toroidal current is less than for the cases in Fig. 2. This is because the attainable toroidal current is proportional to the ratio of the toroidal flux to the injector flux, but this toroidal current does not say how much closed flux current can be achieved in a given CHI configuration as discussed in Ref. [2].

Figure 3 shows the results for cases Q1, Q2 and Q3, in which the electron temperatures are 200 eV, 100 eV and 50 eV, respectively. At lower electron temperature, increased plasma resistivity would allow the injected flux to decay faster and this induces a higher loop voltage. This result suggests that although a lower electron temperature may be more suitable for inducing closed flux formation in TSC simulations, the resulting plasma will also decay away faster, so it will be necessary to increase the plasma electron temperature by some other means (such as for example by ECH heating) to confine the CHI produced closed flux for long durations for eventually coupling the CHI target to other non-inductive current drive methods.

Figure 4 is a plot of the CHI produced toroidal current for all cases. Here it is important to note that most of the CHI produced current in these simulations flows on open field lines. Therefore, the term toroidal current, instead of plasma current, is used to make this distinction clear. The important parameter is the peak toroidal current, which occurs at about 0.7 ms. The persistent toroidal current in these simulations past about 1 ms is not particularly of interest to this study, as they have not been adequately modelled in these initial simulations and will be the subject of future work. For cases Q1 to Q3, the peak toroidal

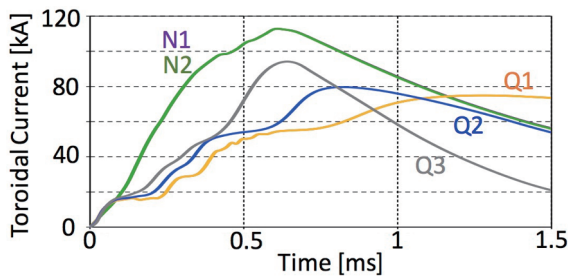


Fig. 4 Time plot of CHI produced toroidal current for cases, N1-2, Q1-3.

current in all cases is much less than for the NSTX-like case, suggesting that QUEST CHI research can benefit if the electrode location is lowered so that it is closer to the PF5-2 coil or possibly through the addition of a new PF coil that is positioned to be closer to the electrode plate.

3. Summary

The first simulations have provided useful guidance for transient CHI experiments on QUEST. First, the results show that in the QUEST-like configuration in which the electrode plate is farther away from the injector coil it may be quite important to energize the PF4-3 coil in order to produce a sufficiently narrow injector flux footprint width so as to induce flux closure. Without the use this coil, the injector flux is simply spread out too widely along the electrode surface, which makes it easy for the injected flux to pull back into the injector after the injector current is reduced to zero.

Second, closer positioning of the electrode plate to the PF5-2 coils allow the injector flux footprints to be more easily controlled. This would suggest the need for some lowering of the electrode plate combined with the use of CHI-specific injector coil or coils as a future modification to the CHI system design on QUEST.

The simulations also show that, in the 2d scenario of TSC, ramping down the injector coil current does not seem to be an important factor for inducing flux closure dur-

ing the very early phase of flux closure. Finally, although flux closure seems easier at lower electron temperatures, the need for a high electron temperature plasma for future sustained non-inductive operation means that a high power ECH system may be necessary to support CHI studies.

As noted in Section 2 and due to the limitations of the present TSC model, it is not useful to make quantitative comparisons of closed flux generation at this stage in these very first simulations of the CHI configuration in QUEST. In addition, the induced loop voltage is not the only mechanism for closed flux generation in CHI plasmas, as indicated by related simulations for the NSTX geometry with the NIMROD code [12, 13].

Acknowledgments

This work is supported by Japan / U. S. Cooperation in Fusion Research and Development, NIFS Collaboration Research Program (NIFS17KUTR130), the Collaborative Research Program of RIAM, Kyushu University (international collaboration frame work No.8 in 2017) and a Grant-in-Aid for JSPS Fellows (KAKENHI Grant Number 16H02441, 24656559). This work is supported by US DOE under the Contracts DE-FG02-99ER54519 and DE-AC02-09CH11466.

- [1] R. Raman *et al.*, Phys. Rev. Lett. **90**, 075005 (2003).
- [2] R. Raman *et al.*, Phys. Plasmas **18**, 092504 (2011).
- [3] K. Hanada *et al.*, Plasma. Fusion. Res. **5**, S1007 (2010).
- [4] K. Hanada *et al.*, Nucl. Fusion **57**, 126061 (2017).
- [5] K. Kuroda *et al.*, Plasma Fusion Res. **12**, 1202020 (2017).
- [6] R. Raman *et al.*, Fusion Sci. Technol. **68**, 674 (2015).
- [7] R. Raman *et al.*, Nucl. Fusion **53**, 073017 (2013).
- [8] H. Idei *et al.*, Nucl. Fusion **57**, 126045 (2017).
- [9] S.C. Jardin, N. Pomphrey and J. Delucia, J. Comput. Phys. **66**, 481 (1986).
- [10] S.C. Jardin *et al.*, Nucl. Fusion **33**, 371 (1993).
- [11] R. Raman *et al.*, Nucl. Fusion **51**, 113018 (2011).
- [12] F. Ebrahimi and R. Raman, Nucl. Fusion **56**, 044002 (2016).
- [13] F. Ebrahimi and R. Raman, Phys. Rev. Lett. **114**, 205003 (2015).
- [14] T.R. Jarboe, Fusion Sci. Technol. **15**, 7 (1989).